



Partitioning, dynamics, and orientation of lung surfactant peptide KL₄ in phospholipid bilayers

Joanna R. Long^{*}, Frank D. Mills, Omjoy K. Ganesh, Vijay C. Antharam, R. Suzanne Farver

Department of Biochemistry and Molecular Biology and McKnight Brain Institute, Box 100245, Gainesville, FL 32610-0245, USA

ARTICLE INFO

Article history:

Received 1 May 2009

Received in revised form 19 August 2009

Accepted 31 August 2009

Available online 6 September 2009

Keywords:

KL₄

Sinapultide

Lucinactant

Lung surfactant

Surfactant protein B

Respiratory distress syndrome

Lipid bilayer

²H NMR

Leucine side chain dynamics

ABSTRACT

Lung surfactant protein B (SP-B) is a lipophilic protein critical to lung function at ambient pressure. KL₄ is a 21-residue peptide which has successfully replaced SP-B in clinical trials of synthetic lung surfactants. CD and FTIR measurements indicate KL₄ is helical in a lipid bilayer environment, but its exact secondary structure and orientation within the bilayer remain controversial. To investigate the partitioning and dynamics of KL₄ in phospholipid bilayers, we introduced CD₃-enriched leucines at four positions along the peptide to serve as probes of side chain dynamics via ²H solid-state NMR. The chosen labels allow distinction between models of helical secondary structure as well as between a transmembrane orientation or partitioning in the plane of the lipid leaflets. Leucine side chains are also sensitive to helix packing interactions in peptides that oligomerize. The partitioning and orientation of KL₄ in DPPC/POPG and POPC/POPG phospholipid bilayers, as inferred from the leucine side chain dynamics, is consistent with monomeric KL₄ lying in the plane of the bilayers and adopting an unusual helical structure which confers amphipathicity and allows partitioning into the lipid hydrophobic interior. At physiologic temperatures, the partitioning depth and dynamics of the peptide are dependent on the degree of saturation present in the lipids. The deeper partitioning of KL₄ relative to antimicrobial amphipathic α -helices leads to negative membrane curvature strain as evidenced by the formation of hexagonal phase structures in a POPE/POPG phospholipid mixture on addition of KL₄. The unusual secondary structure of KL₄ and its ability to differentially partition into lipid lamellae containing varying levels of saturation suggest a mechanism for its role in restoring lung compliance.

© 2009 Elsevier B.V. All rights reserved.

1. Introduction

Lung surfactant is a highly organized, lipid-rich fluid which lines the highly curved alveoli and lowers surface tension. Lung surfactant protein B (SP-B) is an extremely hydrophobic protein which is critical to the proper trafficking of lipids in lung surfactant and establishment of a stable air–water interface [1,2]. Mature SP-B is a homodimer with two 79–81 amino acid disulfide-linked subunits containing high levels of valine, leucine, isoleucine, proline, alanine, phenylalanine,

and tryptophan [3–5]. Each monomer contains an additional six cysteines that form intramolecular disulfide bonds and their pattern of disulfide formation along with lipophilicity place SP-B in the saposin family of proteins. The hydrophobicity and disulfide bridges in SP-B also make purification or heterologous expression of the protein in large quantities impractical. Synthetic, peptide-based lung surfactant replacements for treatment of RDS have shown promise and would remove the immunologic risks associated with current therapies utilizing animal-derived lung surfactant [6–8].

Much of the activity of SP-B in altering lipid organization and dynamics can be recapitulated by the N- and C-terminal 20–25 amino acid fragments of SP-B [4,9]. Both peptides form helices in lipid environments [10–13], but their individual roles in lipid trafficking are not well understood. While both peptides have considerable surface activity, activity similar to native SP-B has only been achieved with a chimeric construct of the two peptides [14]. The C-terminus contains many leucines and lacks aromatic residues while the N-terminus contains four prolines as well as a phenylalanine and a tryptophan. The peptides also have different spacings of hydrophilic and hydrophobic amino acids. These differences could lead to subtle variations in secondary structure and partitioning into lipid lamellae as well as different effects on phospholipid dynamics.

Abbreviations: SP-B, surfactant protein B; RDS, respiratory distress syndrome; TM, transmembrane; NMR, nuclear magnetic resonance; CD, circular dichroism; FTIR, Fourier transform infrared spectroscopy; MLV, multilamellar vesicle; LUV, large unilamellar vesicle; L α , fluid lamellar phase; L β , gel lamellar phase; POPC, 1-palmitoyl-2-oleoyl-*sn*-glycero-3-phosphatidylcholine; POPE, 1-palmitoyl-2-oleoyl-*sn*-glycero-3-phosphatidylethanolamine; POPG, 1-palmitoyl-2-oleoyl-*sn*-glycero-3-phosphatidylglycerol; DPPC, 1,2-dipalmitoyl-*sn*-glycero-3-phosphocholine; P/L, peptide/lipid molar ratio

^{*} Corresponding author. Box 100245, Department of Biochemistry and Molecular Biology, University of Florida, Gainesville, FL 32610-0245, USA. Tel.: +1 352 846 1506; fax: +1 352 392 3422.

E-mail address: jrlong@mbi.ufl.edu (J.R. Long).

The C-terminus of SP-B served as the template for designing the KL₄ peptide, KLLLLKLLLLKLLLLK [8], which to date has shown the greatest clinical success for treatment of respiratory distress syndrome (RDS) with synthetic surfactant [15–19]. The basis for the primary sequence of KL₄ was the charge distribution and hydrophilic/hydrophobic ratio within SP-B_{59–80}. However, their primary sequences have only modest similarity. KL₄ has also been found via CD and FTIR to adopt a helical conformation in a lipid environment [20–22], but the periodicity of the charged lysine residues is at odds with the peptide adopting a canonical α -helical conformation (3.6 residues/turn) which is either amphipathic, for partitioning at the lipid interface, or which can span the lipid bilayer in a TM orientation without burying lysine side chains in the hydrophobic interior of the bilayer. An early FTIR study of KL₄ in DPPC/DPPG concluded the peptide formed a helix spanning the bilayers and posited that KL₄ might more closely mimic lung surfactant protein C (SP-C) rather than the C-terminus of SP-B [20]. More recent IR studies of KL₄ conclude that it binds to the lipid interface but its structure and penetration are lipid and pressure dependent [23]. An assay of the ability of KL₄ to cross ER microsomal membranes via translocon-mediated translation in an in vitro transcription–translation system demonstrated that when KL₄ is expressed within a membrane protein host it can span phospholipid bilayers [24]. While all of these experiments are well suited for analyzing peptides which clearly form amphipathic or TM α -helices, they are inherently low in resolution and are also sensitive to sample conditions (hydration and P/L ratio in the case of FTIR and flanking protein sequences and integrity of the microsomal membranes in the case of the in vitro translation assay). Additionally, many of the published studies have been carried out at room temperature, well below the melting temperature of DPPC (the primary lipid in lung surfactant) or even lung surfactant itself, and with P/L ratios that are much higher than is clinically relevant, raising the possibility of peptide aggregation.

We have been utilizing solid-state NMR spectroscopy to gain a higher-resolution understanding of the structure of KL₄ and its effects on lipid organization under physiologically relevant conditions. In particular, the structure of KL₄ in 4:1 DPPC/POPG and 3:1 POPC/POPG lipid mixtures and its effects on phospholipid dynamics have been characterized. The former lipid composition is similar to formulations commonly used in synthetic lung surfactant, while the latter is a paradigm lipid system commonly employed to probe peptide/lipid interactions, particularly in studies of cationic, amphipathic helices [25–27]. Lipid phases of either of these compositions

could also be found in localized areas of the alveoli during the breathing cycle [28].

With ²H and ³¹P solid-state NMR we have established that the lipids remain in lamellar phases up to 5 mol% KL₄ with no evidence of phase separation at physiologic (37 °C) temperature. The effects of KL₄ on the two lipid systems vary with the fatty acyl chains in the DPPC/POPG mixture becoming more ordered on addition of peptide while the hydrophobic interior of the POPC/POPG bilayers becomes more disordered. Based on order parameter analyses, we interpreted these observations as the peptide partitions more deeply into the DPPC/POPG bilayers [29].

High-resolution measurements on KL₄ in POPC/POPG bilayers via magic angle spinning dipolar recoupling experiments indicate that the peptide adopts an amphipathic helical structure due to the backbone torsion angles diverging from canonical values (e.g., $-\phi$, $-\psi$) in the lipid environment to form a helix with a lower angle of rotation per residue and (ϕ , ψ) torsion angles that average (-105° , -30°) [22]. More recent measurements on KL₄ in DPPC/POPG suggest that the peptide can form a helix which has an even lower angle of rotation, increasing its amphipathicity, and allowing it to more deeply partition into the lipid interior without adopting a TM orientation (Fig. 1C; A.K. Mehta and J.R. Long, submitted for publication). However, these measurements rely on determining the relative orientations of ¹³C' chemical shift anisotropy tensors, which have degeneracies in particular regions of (ϕ , ψ) space, making it difficult to distinguish between a canonical α -helix (-63° , -45°) and a more amphipathic helix (-63° , -81°). Molecular dynamics simulations, coupled with ssNMR measurements of inter-residue ¹³C'→¹⁵N distances and CD spectra, indicate that the (-63° , -81°) conformation is correct, but more conclusive data are needed. Additionally, the orientation of the KL₄ helix relative to the bilayer normal in DPPC/POPG lipids cannot be conclusively determined from the lipid dynamics measurements. Moreover, structural characterization via dipolar recoupling experiments requires the removal of dynamics, via flash-freezing and lyophilization, removing any information on the dynamics of the peptide which might be important to its function.

Based on the helical models for KL₄ in DPPC/POPG and POPC/POPG (Fig. 1), we chose to examine the side chain dynamics of four leucines in KL₄ as a function of temperature and lipid composition. The four positions were selected to be sensitive to both helix pitch and the orientation of KL₄ within the lipid bilayers as well as to provide insight into how the dynamics of the peptide might play a role in its function. Leucine residue dynamics are also sensitive to

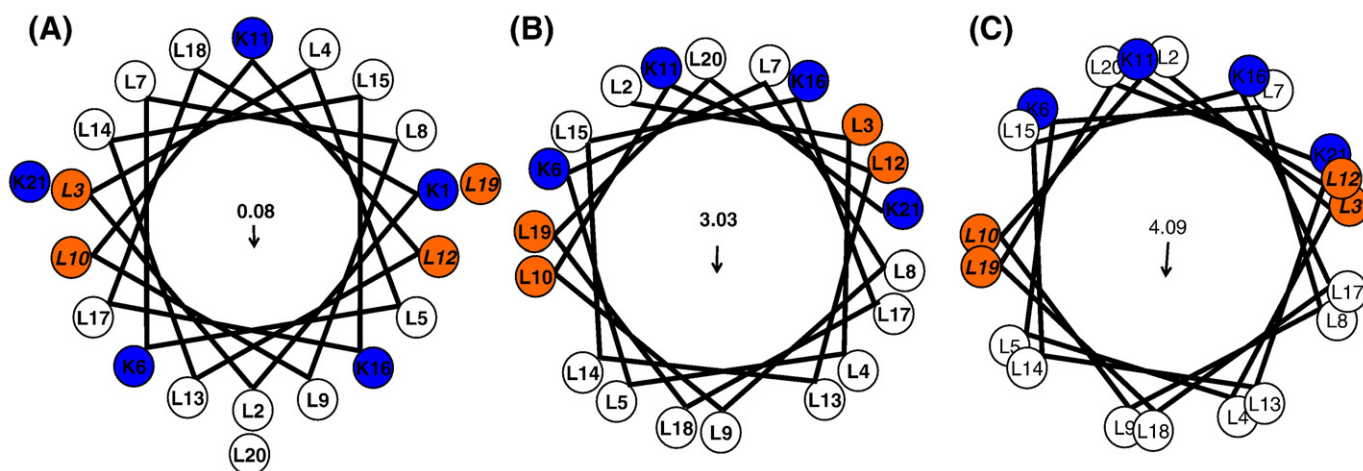


Fig. 1. Helical wheel plots of KL₄ with varying (ϕ , ψ) torsion angles. (A) Wheel generated assuming a canonical α -helix (ϕ , $\psi = -63^\circ$, -42°); (B) using the average torsion angles determined in POPC/POPG vesicles (ϕ , $\psi = -105^\circ$, -30°); and (C) using the average torsion angles observed in DPPC/POPG vesicles (ϕ , $\psi = -63^\circ$, -81°). Arrows indicate the net hydrophobic moments resulting from the distribution of charged lysine side chains on the helix surface. The first lysine is not shown in (B) and (C) as NMR data indicate that the N-terminus is less structured relative to the rest of the helix.

peptide oligomerization [30], allowing us to determine whether KL₄ is monomeric under physiologically relevant conditions. This is particularly of interest given the propensity of leucine residues to enhance peptide oligomerization in membranes [31,32]. Variations in temperature allow us to monitor the partitioning of KL₄ in both fluid- and gel-phase lipid bilayers to infer how its structure, orientation, and organization might vary between the different sample conditions used in previous studies.

A particular advantage of probing peptide dynamics via ²H NMR is that it enables us to study KL₄ under close to physiologic conditions, with full hydration of the lipids, and over a range of temperatures relevant to the phase properties of the lipids. This allows us to assay whether structural measurements, carried out on samples in which dynamics are removed by flash-freezing samples and subsequent lyophilization, are consistent with the structure and dynamics of the peptide under more physiologically relevant conditions. It also allows us to monitor the interplay between peptide partitioning, lipid dynamics, peptide secondary structure and dynamics, lipid polymorphisms, and temperature, providing important insights into lung surfactant function and more generally the enthalpic and entropic contributions underlying amphipathic peptides interactions with and influence on phospholipid assemblies.

2. Materials and methods

2.1. Synthesis of KL₄

Selectively deuterated 5-*d*₃-L-leucine was purchased (Cambridge Isotopes, Andover, MA) and fmoc-protected using standard protocols [33]. Four variants of KL₄, each containing a single enriched leucine (at Leu3, Leu10, Leu12, or Leu19), were synthesized via solid-phase peptide synthesis on a Wang resin (ABI 430, ICBR, UF), cleaved from the resin with 90% TFA/5% triisopropyl-silane/5% water and ether precipitated. The cleaved product was purified via RP-HPLC using a C18 Vydac column with a water/acetonitrile gradient (containing 0.3% TFA). The fractions corresponding to KL₄ were collected, and the purity of the product was verified by mass spectrometry with a single species of MW = 2572. Dried peptide was weighed and dissolved in methanol to a stock concentration of approximately 1 mM, and aliquots were analyzed by amino acid analysis for a more accurate determination of concentration and to verify purity (Molecular Structure Facility, UC Davis).

2.2. Preparation of peptide: lipid samples

POPC, DPPC, and POPG were purchased as chloroform solutions (Avanti Polar Lipids, Alabaster, AL) and concentrations were verified by phosphate analysis [34] (Bioassay Systems, Hayward, CA). The lipids were mixed at a molar ratio of 4:1 DPPC/POPG and 3:1 POPC/POPG in chloroform and aliquoted. For samples containing peptide, a methanol solution of KL₄ was added to lipid solutions with final protein/lipid (P/L) molar ratio of 1:50 to match the clinical formulation of KL₄. The samples were dried under a stream of nitrogen with the sample temperature maintained at 42–50 °C in a water bath; the resulting films were suspended in warm cyclohexane, flash-frozen, and lyophilized overnight to remove residual solvent.

2.3. Solid-state NMR analysis

For each solid-state NMR sample, 20–30 mg of peptide–lipid powder was placed in a 5 mm diameter NMR tube and 200 μL of buffer containing 5 mM HEPES at pH 7.4, 140 mM NaCl, and 1 mM EDTA in ²H depleted water (Cambridge Isotopes, Andover, MA) was added. NMR samples were then subjected to 3–5 freeze–thaw cycles with gentle manual agitation to form MLVs. ²H NMR data were collected on a 500 MHz Bruker Avance system (Billerica, MA) using a standard

high resolution 5 mm broadband probe and a quad-echo sequence (90°–τ–90°–τ–acq with τ = 30 μs) with a B₁ field of 40 kHz. Spectra were acquired with 100,000–400,000 transients, a 0.2-second recycle delay time, and 500 kHz sweep width. Prior to Fourier transformation, spectra were phased, symmetrized by adding the complex conjugate, and damped with 200 Hz exponential line broadening (or 500 Hz for low signal spectra at the lowest temperature), with removal of signal between ±200 Hz (±500 Hz) ascribed to residual ²H₂O. Spectra were acquired over a temperature range of –10 to 40 °C. Unsymmetrized spectra without solvent removal are available in the [Supplementary Data](#). ³¹P NMR data were collected on a 600 MHz Bruker Avance system (Billerica, MA) using a standard 5 mm BBO probe. Proton decoupling (25 kHz) was employed during acquisition to remove dipolar couplings. Spectra were acquired with 512–1024 scans and a 5-second recycle delay between scans to minimize RF sample heating. Chemical shift referencing is relative to an external phosphate buffer standard.

3. Results

3.1. Leucine side chain dynamics for KL₄ in POPC/POPG lipid vesicles

²H solid-state NMR spectra for Leu3, Leu10, Leu12, and Leu19 in 3:1 POPC/POPG as a function of temperature and label position are shown in [Figs. 2 and 3](#). First moment analyses of the spectra are provided in the [Supplementary Data](#). The gel→liquid crystalline phase transition temperature of this lipid mixture is –3 °C. At temperatures near the phase transition temperature, the Leu3 and Leu12 positions exhibit less dynamics relative to the Leu10 and Leu19 positions. The breadth and shape of the Leu3 and Leu12 powder patterns at –10 °C are consistent with the deuterated leucine methyl groups solely undergoing 3-fold rotation about the C_γ–C_δ bond; the Leu10 and Leu12 line shapes are consistent with additional motion about the C_β–C_γ and/or C_α–C_β bonds [30,35,36]. At 0 °C, the Leu3 and Leu12 positions begin to exhibit dynamics about the C_β–C_γ or C_α–C_β bonds, but they are more limited relative to the Leu10 and Leu19 positions. In contrast, at 14 °C, the line shapes for Leu3, Leu12, and Leu19 have significantly narrowed relative to the Leu10 position. The dissimilarity in dynamics of the Leu10 and Leu12 residues as well as the differences between Leu3 and Leu19 clearly rule out a TM orientation in the POPC/POPG lipid bilayers at all the monitored temperatures. Due to the phase transition temperature of the lipids being similar to the freezing point of water, with significant dynamics remaining only in the hydrophobic interior of the lipid bilayers at –10 °C, we interpret the contrast in dynamics between Leu3 and Leu10 relative to Leu12 and Leu19 as a function of temperature as the Leu3 and Leu10 positions partitioning closer to the lipid/water interface while the Leu12 and Leu19 positions partition more deeply into the hydrophobic interior of the lipid bilayers. The correlation of dynamics between the Leu10 and Leu19 positions as well as between the Leu12 and Leu3 positions is also more consistent with the helical model shown in [Fig. 1C](#) rather than a canonical α-helix ([Fig. 1A](#)), which would predict correlations between Leu3 and Leu10 and between Leu12 and Leu19 if the helix axis lie in the plane of the lipid leaflet.

At higher temperatures (14 and 25 °C), the Leu3, Leu12, and Leu19 spectra exhibit line shapes consistent with more motion about the C_β–C_γ and/or C_α–C_β bonds, while the Leu10 position still exhibits limited dynamics. This is consistent with the Leu10 position partitioning more deeply into the lipid interior while the Leu3, Leu12, and Leu19 residues partition at the lipid interface and is predicted by the helical structure observed for KL₄ at ambient temperatures in POPC/POPG vesicles ([Fig. 1B](#)). At 40 °C, a small decrease in dynamics is observed for the Leu19 position while the Leu3 and Leu12 positions continue to show more motion. This is consistent with the peptide partitioning slightly deeper into the lipid

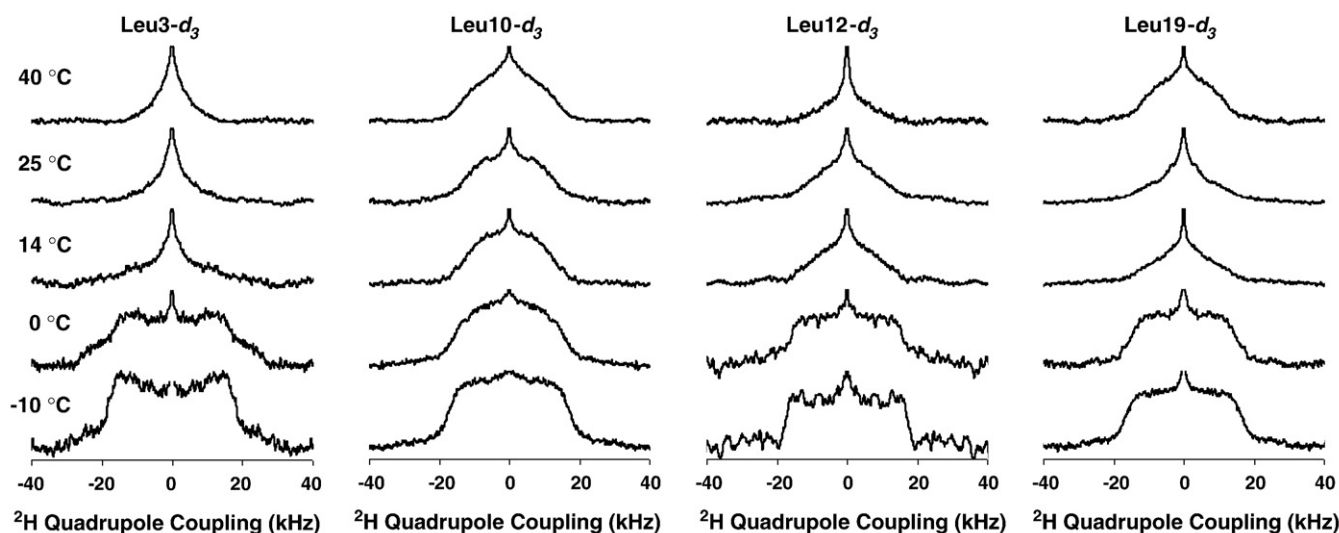


Fig. 2. Deuterium NMR spectra as a function of temperature for the various 5- d_3 -L-leucine enriched position in KL₄ in samples containing POPC/POPG vesicles.

interior, an entropically driven process due to the hydrophobicity of KL₄, resulting in a small change in helix pitch and subsequent increase in hydrophobic moment, as in the model shown in Fig. 1C.

3.2. Leucine side chain dynamics for KL₄ in DPPC/POPG lipid vesicles

^2H solid-state NMR spectra for Leu3, Leu10, Leu12, and Leu19 in 4:1 DPPC/POPG as a function of temperature and label position are shown in Fig. 4; first moment analyses are provided in the Supplementary Data. The gel→liquid crystalline phase transition of this lipid mixture is at 36 °C [29]. Below the phase transition temperature (e.g., 25 °C), all four positions exhibit decreased dynamics consistent with the methyl groups undergoing 3-fold rotation about the $\text{C}_\gamma\text{--}\text{C}_\delta$ bond and limited motion about the $\text{C}_\beta\text{--}\text{C}_\gamma$ and/or $\text{C}_\alpha\text{--}\text{C}_\beta$ bonds. The dynamics of the Leu12 position is slightly less restricted than that of the Leu19 position, for which the spectrum has a lower first moment than the Leu3 and Leu10 positions, consistent with differences in partitioning. The dynamics of all four positions is similar to that seen in 3:1 POPC/POPG lipids at lower temperatures, as would be expected given the differences in the phase transition temperatures of the lipids.

Above the phase transition (40 °C), the Leu3 and Leu12 side chains are much more dynamic while the Leu10 and Leu19 positions continue to exhibit only limited dynamics. The dissimilarity in dynamics of the Leu10 and Leu12 residues as well as the differences between Leu3 and Leu19 also clearly rule out a TM orientation in DPPC/POPG lipids. The change in the relative dynamics of the four positions with the phase of the phospholipids suggests changes in the partitioning and/or secondary structure of KL₄ with temperature and underscores the need to study KL₄ at physiologically relevant temperatures, particularly in DPPC-rich mixtures given its high transition temperature. The reduced dynamics at the Leu10 and Leu19 positions suggests that they are partitioned into the hydrophobic interior of the lipid bilayers. The correlation of dynamics between the Leu10 and Leu19 positions as well as between the Leu12 and Leu3 positions is again more consistent with the helical models shown in Fig. 1C rather than a canonical α -helix (Fig. 1A) or the helix modeled in Fig. 1B. The dynamics at 40 °C for all four positions in DPPC/POPG is attenuated relative to in POPC/POPG, consistent with the peptide partitioning more deeply into the DPPC/POPG hydrophobic interior as was previously inferred by examining the dynamics of the fatty acyl chains [29].

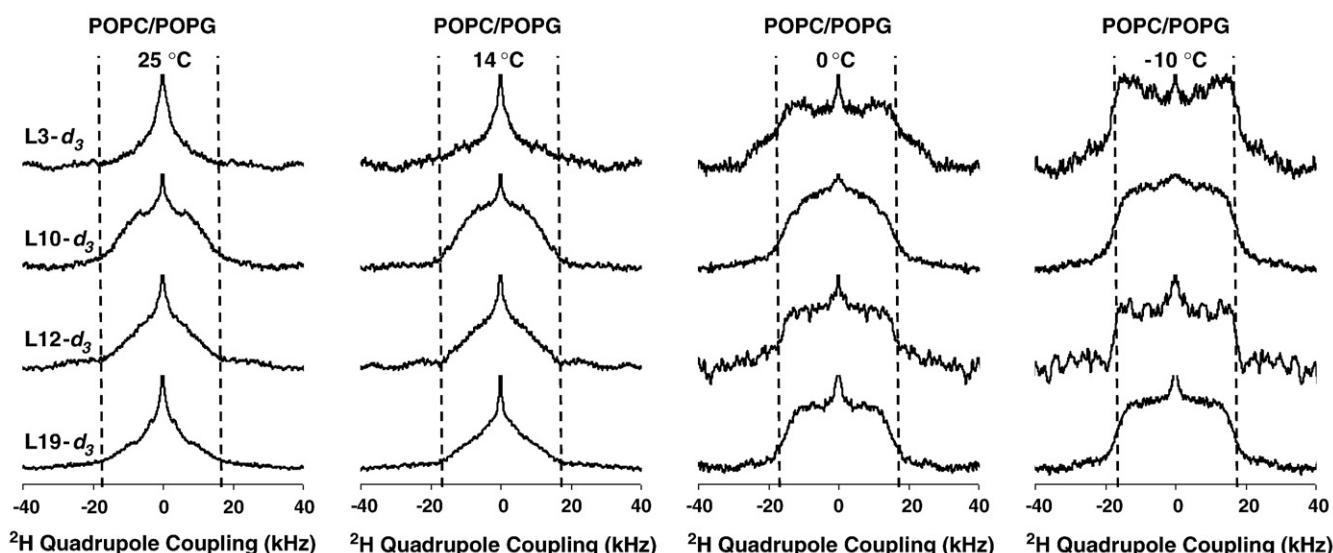


Fig. 3. Deuterium NMR spectra as a function of label position for the various 5- d_3 -L-leucine enriched position in KL₄ in samples containing POPC/POPG vesicles.

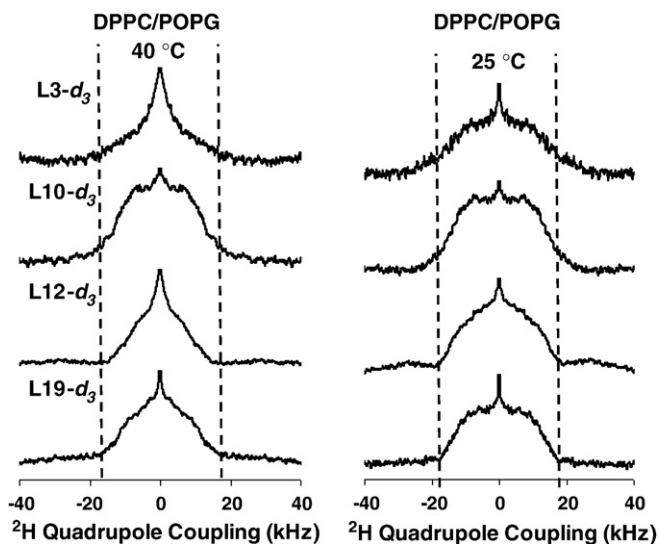


Fig. 4. Deuterium NMR spectra as a function of label position for the various 5- d_3 -L-leucine enriched position in KL₄ in samples containing DPPC/POPG vesicles.

3.3. Partitioning of KL₄ into POPE/POPG lipid vesicles induces negative curvature strain

³¹P solid-state NMR spectra of 3:1 POPE/POPG MLVs with and without 3 mol% KL₄ are shown as a function of temperature in Fig. 5. At lower temperatures, the spectra are indicative of lamellar lipid structures. The average head group orientations of the PE and PG lipids relative to the membrane normal are similar, leading to a single lamellar line shape for the mixture. For the sample containing only phospholipids, the MLVs align significantly in the strong magnetic field leading to a very strong signal at the perpendicular edge of the line shape and almost no signal at the parallel edge. Addition of KL₄ leads to less lipid alignment and a more typical lamellar line shape. The alignment of phospholipid vesicles at the field strengths utilized and the disruption of this alignment by KL₄ have been previously documented [29]. At higher temperatures, the phospholipids undergo a transition to an isotropic phase, as evidenced by the appearance of a resonance near 0 ppm at 55 °C for the sample containing only phospholipids. This transition is complete by 61 °C and further changes in the line shape are not observed. However, for the POPE/POPG sample containing KL₄, the transition from a lamellar phase does not occur until above 61 °C, and the appearance of two separate spectral features is observed at 67 °C. The peak near 0 ppm is consistent with an isotropic phase, while the feature observed at −4 ppm is suggestive of an inverted hexagonal phase. Heating further to 80 °C confirms the formation of hexagonal phase structures with a clear spectral line shape that is reversed relative to the lamellar line shape and half its width. A significant fraction of the phospholipids remain in the isotropic phase, which can be expected given the high percentage of POPG in the sample and the relatively low concentration of KL₄ relative to the phospholipids. The induction of hexagonal phase structures in POPE/POPG mixtures by KL₄ demonstrates that the peptide induces negative membrane curvature strain.

4. Discussion

Models for KL₄ secondary structure and partitioning into lipid bilayers are presented in Fig. 6 [37]. Four possibilities are shown: an α -helix lying in the plane of the bilayers; an α -helix spanning the bilayer; an alternative helical structure, based on our NMR measurements of KL₄ in DPPC/POPG, lying in the plane of the bilayers; and the alternative helical structure spanning the bilayer. The 21-residue

length of the KL₄ peptide is sufficient for it to span the lipid bilayers in a TM orientation, but it would require the burying of 2–3 lysine side chains into the hydrophobic interior. While lysines have a lower energetic barrier for partitioning into lipid bilayers than other basic residues, a TM orientation is only possible if the hydrophobic interaction of the leucine side chains and the overall secondary structure overcome this barrier. Previous studies of peptides containing similar percentages of leucines and lysines indicate that a stable TM orientation can only be achieved when the lysines are distributed closer to the N- and C-termini [38]. Nonetheless, a recent in vitro transcription–translation assay found KL₄ is able to cross the membrane [24]. However, this assay relies on the integration of KL₄ into the *Escherichia coli* inner membrane protein leader peptidase (Lep), which is translated in ER-derived microsomal membranes and the resulting protein is assayed for glycosylation after proteinase K digestion. The assay is problematic in two regards. First, the flanking sequences of the Lep protein may influence the secondary structure of the integrated peptide. Second, KL₄ is known to influence lipid dynamics and trafficking and thus may affect the integrity of the microsomal membranes. Assuming an α -helical conformation, KL₄ possesses a low hydrophobic moment and the predicted ΔG_{app} for the KL₄ sequence inserting into ER membranes is −2.14 kcal/mol [24]. Conversely, if KL₄ assumes a structure with a lower helical pitch, its hydrophobic moment is increased by 3–4 kcal/mol and its insertion in a TM orientation is much less favorable (Fig. 1B or C). Our structural studies of KL₄ interacting with POPC/POPG and DPPC/POPG vesicles suggest that this latter scenario is correct for the peptide under fully hydrated conditions.

An alternative means to assay the orientation of KL₄ in lipid bilayers as well as its partitioning behavior is to examine the dynamics of the leucine side chains at various positions in the peptide. The nonperturbing nature of incorporating ²H into 5- d_3 -L-leucine and the increased sensitivity for ²H solid-state NMR due to the three-fold rotation of the methyl group make this a particularly attractive probe for assaying dynamics. Previously, deuterated leucine has been utilized for examining dynamics and oligomerization of transmembrane sequences [30,35,36]. However, to our knowledge, it has not been used to examine the partitioning of amphipathic helices into lipid bilayers. The frequency and symmetry of the leucines in the KL₄ sequence make the identification of a

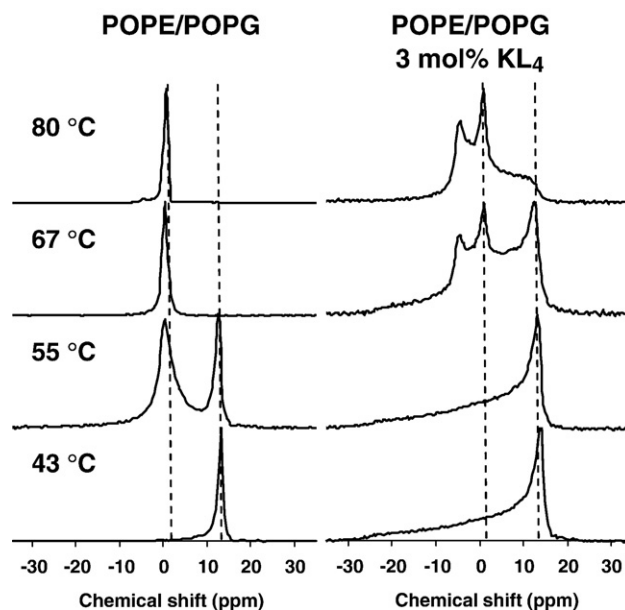


Fig. 5. Phosphorous NMR spectra as a function of temperature for 3:1 POPE/POPG lipid vesicles with and without 3 mol% KL₄.

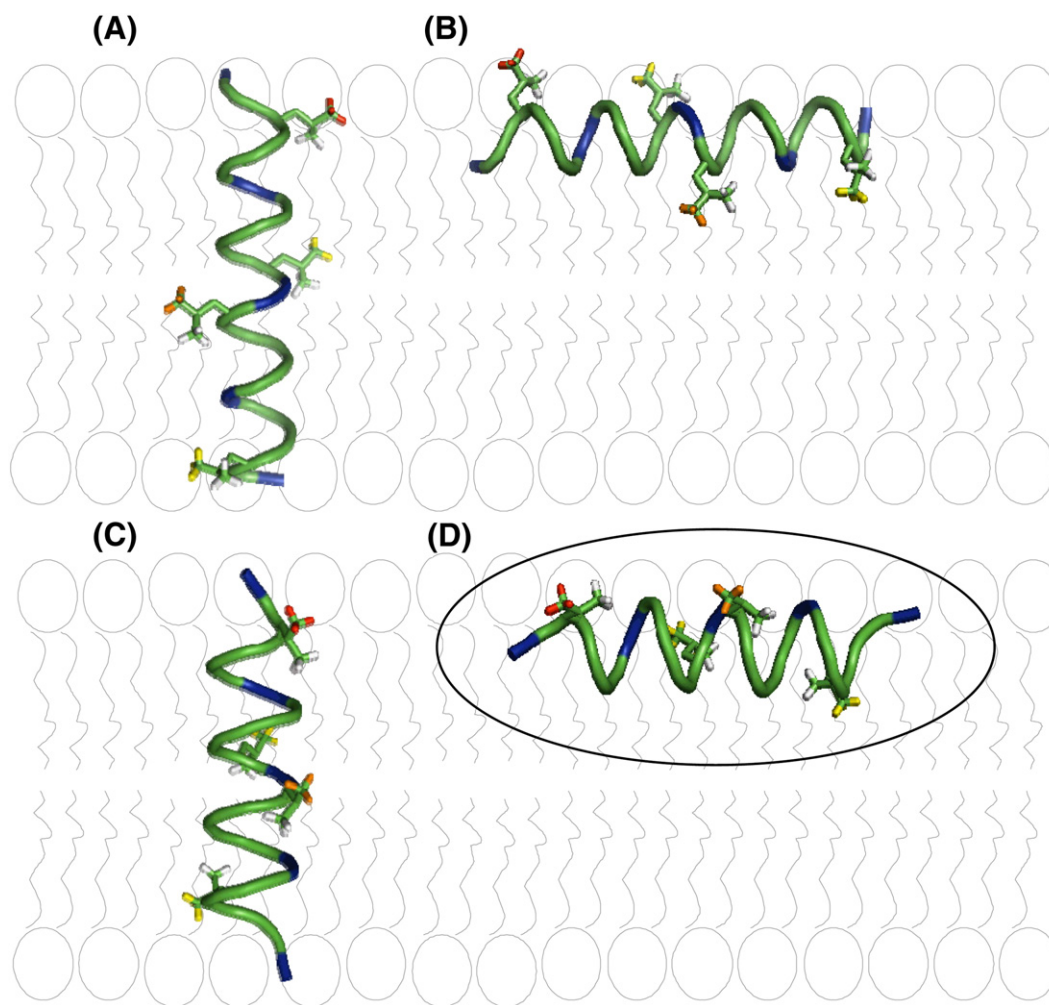


Fig. 6. Model of the possible structures and orientations of KL₄ in the lipid bilayer: (A) a canonical α -helix in a transmembrane orientation; (B) an α -helix in the plane of the bilayer; (C) the helix from Fig. 1C in a transmembrane orientation; and (D) the helix from Fig. 1C lying in the plane of the bilayer. The deuterated leucine methyl groups used in this study are color-coded with respect to their relative dynamics in POPC/POPG at 40 °C with Leu3 (red) > Leu 12 (orange) > Leu10 \approx Leu19 (yellow).

minimal number of sites for labeling particularly straightforward. To assay the orientation of the peptide, we chose two sites at the N- and C-termini (Leu3 and Leu19) as well as two sites which would be located near the center of the bilayer in a TM orientation (Leu10 and Leu12). Under all experimental conditions, the relative dynamics of these positions suggests that a TM orientation is unlikely, particularly since the dynamics of Leu10 and Leu12 differs significantly. While packing of peptide helices in aggregates could lead to differences between these two positions, we do not see a loss of motion about the C_{β} – C_{γ} and/or C_{α} – C_{β} bonds at any of the observed positions as would be expected for helix–helix packing interactions. Additionally, the dynamics observed at the various temperatures was easily reproduced regardless of the order in which spectra were collected consistent with all changes in dynamics being reversible and the samples being fully equilibrated.

Leucine side chains are particularly sensitive to packing of side chains at helix interfaces. While we did not assay all possible helix interfaces in this study, the labels chosen lie at expected interfaces if the peptide were to oligomerize in the plane of the membrane. Above the gel→liquid crystalline phase transition temperature of the lipids, all samples exhibited leucine side chain dynamics about the C_{β} – C_{γ} and/or C_{α} – C_{β} bonds. This is in contrast to what has been observed for leucines found at helix interfaces [30]. In our studies we have found KL₄ to form consistent secondary structure in phospholipids mixtures up to P/L ratios of 1:30. At 1:20, CD and FTIR spectra indicate the

formation of β -sheet type structures consistent with aggregation of the peptide (K. Seu and S Decatur, personal communication).

As can be seen in Fig. 1, differences in helix pitch lead to differences in the expected correlations between the labeled positions for the peptide lying in the plane of the lipid bilayer. For DPPC/POPG and POPC/POPG lipid mixtures near physiologic temperature, the correlation in side chain dynamics among the four observed positions is consistent with a peptide having a high hydrophobic moment (Fig. 1C), which agrees well with our structural measurements carried out on KL₄ in DPPC/POPG lipid vesicles (A.K. Mehta and J.R. Long, submitted for publication). Near room temperature, the dynamics observed for KL₄ in POPC/POPG lipid vesicles correlate with the helical structure previously determined under the same conditions [22]. Based on these observations, only one of the four models in Fig. 5 is consistent with our data near physiologic temperature, as indicated.

In this study, the dynamics observed for the KL₄ leucine side chains in DPPC/POPG-containing samples is significantly attenuated relative to the POPC/POPG-containing samples. This is consistent with previous observations that addition of peptide lowers the acyl chain order parameters in POPC/POPG lipid bilayers but increases the acyl chain order parameters in DPPC/POPG lipid bilayers [29]. This variation in partitioning depth is likely due to the unusual periodicity of the hydrophilic residues which confer temperature-dependent helical plasticity on partitioning of the peptide into lipid bilayers with varying levels of saturation.

Lipid polymorphisms that change the geometry and arrangement of lipid assemblies may be critical for lipid adsorption at the alveolar air–fluid interface [39]. The enrichment of DPPC at the air–water interface has been postulated as one of the major roles of SP-B. The KL₄ peptide's structural plasticity and variable penetration depth can affect the stability and composition of lung surfactant lipid structures by causing negative curvature strain as we have demonstrated in POPE/POPG phospholipid mixtures. These changes in curvature strain provide a mechanism for lipid trafficking from lamellar bodies and tubular myelin to the air–water interface in a manner that may select for DPPC.

Acknowledgements

The assistance of Dr. Alfred Chung in peptide synthesis and of the Molecular Structure Facility at University of California, Davis in AAA analysis is gratefully acknowledged. The research herein was funded by NIH 1R01HL076586 awarded to JRL. Support from the NSF National High Magnetic Field Laboratory and University of Florida is also gratefully acknowledged.

Appendix A. Supplementary data

Supplementary data associated with this article can be found, in the online version, at [doi:10.1016/j.bbamem.2009.08.020](https://doi.org/10.1016/j.bbamem.2009.08.020).

References

- [1] L.M. Nogue, D.E. Demello, L.P. Dehner, H.R. Colten, Brief report – deficiency of pulmonary surfactant protein-B in congenital alveolar proteinosis, *N. Engl. J. Med.* 328 (1993) 406–410.
- [2] J.C. Clark, S.E. Wert, C.J. Bachurski, M.T. Stahlman, B.R. Stripp, T.E. Weaver, J.A. Whitsett, Targeted disruption of the surfactant protein B gene disrupts surfactant homeostasis, causing respiratory failure in newborn mice, *Proc. Natl. Acad. Sci.* 92 (1995) 7794–7798.
- [3] V.K. Sarin, S. Gupta, T.K. Leung, V.E. Taylor, B.L. Ohning, J.A. Whitsett, J.L. Fox, Biophysical and biological activity of a synthetic 8.7-kDa hydrophobic pulmonary surfactant protein SP-B, *Proc. Natl. Acad. Sci.* 87 (1990) 2633–2637.
- [4] S.D. Revak, T.A. Merritt, M. Hallman, G. Heldt, R.J. Lapolla, K. Hoey, R.A. Houghten, C.G. Cochrane, The use of synthetic peptides in the formation of biophysically and biologically-active pulmonary surfactants, *Pediatr. Res.* 29 (1991) 460–465.
- [5] J. Johansson, T. Curstedt, Molecular structures and interactions of pulmonary surfactant components, *Eur. J. Biochem.* 244 (1997) 675–693.
- [6] I. Mingarro, D. Lukovic, M. Vilar, J. Perez-Gil, Synthetic pulmonary surfactant preparations: new developments and future trends, *Curr. Med. Chem.* 15 (2008) 393–403.
- [7] S.L. Seurnyck, J.A. Patch, A.E. Barron, Simple, helical peptoid analogs of lung surfactant protein B, *Chem. Biol.* 12 (2005) 77–88.
- [8] C.G. Cochrane, S.D. Revak, Pulmonary surfactant protein B (SP-B): structure–function relationships, *Science* 254 (1991) 566–568.
- [9] A. Waring, H.W. Taesch, Interactions of surfactant peptides, SP-B and SP-C, with phospholipids using phospholipid spin labels, *Clin. Res.* 37 (1989) A211.
- [10] R. Bruni, H.W. Taesch, A.J. Waring, Surfactant protein-B–lipid interactions of synthetic peptides representing the amino-terminal amphipathic domain, *Proc. Natl. Acad. Sci.* 88 (1991) 7451–7455.
- [11] J.H. Kang, M.K. Lee, K.L. Kim, K.S. Hahn, The relationships between biophysical activity and the secondary structure of synthetic peptides from the pulmonary surfactant protein SP-B, *Biochem. Mol. Biol. Int.* 40 (1996) 617–627.
- [12] V. Booth, A.J. Waring, F.J. Walther, K.M.W. Keough, NMR structures of the C-terminal segment of surfactant protein B in detergent micelles and hexafluoro-2-propanol, *Biochemistry* 43 (2004) 15187–15194.
- [13] M. Sarker, A.J. Waring, F.J. Walther, K.M.W. Keough, V. Booth, Structure of mini-B, a functional fragment of surfactant protein B, in detergent micelles, *Biochemistry* 46 (2007) 11047–11056.
- [14] A.J. Waring, F.J. Walther, L.M. Gordon, J.M. Hernandez-Juviel, T. Hong, M.A. Sherman, C. Alonso, T. Alig, A. Braun, D. Bacon, J.A. Zasadzinski, The role of charged amphipathic helices in the structure and function of surfactant protein B, *J. Pept. Res.* 66 (2005) 364–374.
- [15] C.G. Cochrane, S.D. Revak, A. Merritt, G.P. Heldt, M. Hallman, M.D. Cunningham, D. Easa, A. Pramanik, D.K. Edwards, M.S. Alberts, The efficacy and safety of KL₄-surfactant in infants with respiratory distress syndrome, *Am. J. Respir. Crit. Care Med.* 153 (1996) 404–410.
- [16] C.G. Cochrane, S.D. Revak, T.A. Merritt, I.U. Schraufstatter, R.C. Hoch, C. Henderson, S. Andersson, H. Takamori, Z.G. Oades, Bronchoalveolar lavage with KL₄-surfactant in models of meconium aspiration syndrome, *Pediatr. Res.* 44 (1998) 705–715.
- [17] T.E. Wiswell, R.M. Smith, L.B. Katz, L. Mastroianni, D.Y. Wong, D. Willms, S. Heard, M. Wilson, R.D. Hite, A. Anzueto, S.D. Revak, C.G. Cochrane, Bronchopulmonary segmental lavage with surfaxin (KL₄-surfactant) for acute respiratory distress syndrome, *Am. J. Respir. Crit. Care Med.* 160 (1999) 1188–1195.
- [18] S.K. Sinha, T. Lacaze-Masmonteil, A.V.I. Soler, T.E. Wiswell, J. Gadzinowski, J. Hajdu, G. Bernstein, R. d'Agostino, S.T.A.R. Dist, A multicenter, randomized, controlled trial of lucinactant versus poractant alfa among very premature infants at high risk for respiratory distress syndrome, *Pediatrics* 115 (2005) 1030–1038.
- [19] M. Ghodrati, Lung surfactants, *Am. J. Health-Syst. Pharm.* 63 (2006) 1504–1521.
- [20] M. Gustafsson, G. Vandenbussche, T. Curstedt, J.M. Ruysschaert, J. Johansson, The 21-residue surfactant peptide (LysLeu)₄Lys (KL₄) is a transmembrane alpha-helix with a mixed nonpolar/polar surface, *FEBS Lett.* 384 (1996) 185–188.
- [21] A. Saenz, O. Canadas, L.A. Bagatolli, M.E. Johnson, C. Casals, Physical properties and surface activity of surfactant-like membranes containing the cationic and hydrophobic peptide KL₄, *FEBS J.* 273 (2006) 2515–2527.
- [22] F.D. Mills, V.C. Antharam, O.K. Ganesh, D.W. Elliott, S.A. McNeill, J.R. Long, The helical structure of surfactant peptide KL₄ when bound to POPC:POPG lipid vesicles, *Biochemistry* 47 (2008) 8292–8300.
- [23] P. Cai, C.R. Flach, R. Mendelsohn, An infrared reflection–absorption spectroscopy study of the secondary structure in (KL₄)₄K, a therapeutic agent for respiratory distress syndrome, in aqueous monolayers with phospholipids, *Biochemistry* 42 (2003) 9446–9452.
- [24] L. Martinez-Gil, J. Perez-Gil, I. Mingarro, The surfactant peptide KL₄ sequence is inserted with a transmembrane orientation into the endoplasmic reticulum membrane, *Biophys. J.* 95 (2008) L36–L38.
- [25] E. Terzi, G. Holzemann, J. Seelig, Interaction of Alzheimer beta-amyloid peptide (1–40) with lipid membranes, *Biochemistry* 36 (1997) 14845–14852.
- [26] A. Ramamoorthy, S. Thennarasu, D.K. Lee, A. Tan, L. Maloy, Solid-state NMR investigation of the membrane-disrupting mechanism of antimicrobial peptides MSI-78 and MSI-594 derived from magainin 2 and melittin, *Biophys. J.* 91 (2006) 206–216.
- [27] T. Wieprecht, O. Apostolov, M. Beyermann, J. Seelig, Thermodynamics of the alpha-helix–coil transition of amphipathic peptides in a membrane environment: implications for the peptide–membrane binding equilibrium, *J. Mol. Biol.* 294 (1999) 785–794.
- [28] R. Veldhuizen, K. Nag, S. Orgeig, F. Possmayer, The role of lipids in pulmonary surfactant, *BBA-Mol. Basis Dis.* 1408 (1998) 90–108.
- [29] V.C. Antharam, D.W. Elliott, F.D. Mills, R.S. Farver, E. Sternin, J.R. Long, The penetration depth of surfactant peptide KL₄ into membranes is determined by fatty acid saturation, *Biophys. J.* 96 (2009) 4085–4098.
- [30] W.W. Ying, S.E. Irvine, R.A. Beekman, D.J. Siminovich, S.O. Smith, Deuterium NMR reveals helix packing interactions in phospholamban, *J. Am. Chem. Soc.* 122 (2000) 11125–11128.
- [31] L.M. Gottler, R.D. Bea, C.E. Shelburne, A. Ramamoorthy, E.N.G. Marsh, Using fluorine amino acids to probe the effects of changing hydrophobicity on the physical and biological properties of the beta-hairpin antimicrobial peptide protegrin-1, *Biochemistry* 47 (2008) 9243–9250.
- [32] L.M. Gottler, H.Y. Lee, C.E. Shelburne, A. Ramamoorthy, E.N.G. Marsh, Using fluorine amino acids to modulate the biological activity of an antimicrobial peptide, *ChemBioChem* 9 (2008) 370–373.
- [33] M. Samuel-Landtiser, C. Zachariah, C.R. Williams, A.S. Edison, J.R. Long, Incorporation of isotopically enriched amino acids, *Curr. Protoc. Protein Sci.* (2007) (Chapter 26, Unit 26 3).
- [34] P.S. Chen, T.Y. Toribara, H. Warner, Microdetermination of phosphorus, *Anal. Chem.* 28 (1956) 1756–1758.
- [35] E.K. Tiburu, E.S. Karp, P.C. Dave, K. Damodaran, G.A. Lorigan, Investigating the dynamic properties of the transmembrane segment of phospholamban incorporated into phospholipid bilayers utilizing H-2 and N-15 solid-state NMR spectroscopy, *Biochemistry* 43 (2004) 13899–13909.
- [36] S. Abu-Baker, J.X. Lu, S.D. Chu, C.C. Brinn, C.A. Makarov, G.A. Lorigan, Side chain and backbone dynamics of phospholamban in phospholipid bilayers utilizing H-2 and N-15 solid-state NMR spectroscopy, *Biochemistry* 46 (2007) 11695–11706.
- [37] W.L. DeLano, DeLano Scientific, LLC, Palo Alto, CA, USA 2008.
- [38] B. Vogt, P. Ducarme, S. Schinzel, R. Brasseur, B. Bechinger, The topology of lysine-containing amphipathic peptides in bilayers by circular dichroism, solid-state NMR, and molecular modeling, *Biophys. J.* 79 (2000) 2644–2656.
- [39] W.R. Perkins, R.B. Dause, R.A. Parente, S.R. Minchey, K.C. Neuman, S.M. Gruner, T.F. Taraschi, A.S. Janoff, Role of lipid polymorphism in pulmonary surfactant, *Science* 273 (1996) 330–332.